Microburst Scale Size Derived from Multiple Bounces of a Microburst Simultaneously Observed with the FIREBIRD-II CubeSats

Mykhaylo Shumko[1], John Sample[1], Arlo Johnson[1], Bern Blake[2], Alex Crew[3], Harlan Spence[4], David Klumpar[1], Oleksiy Agapitov[5], Matthew Handley[1]

[1]Department of Physics, Montana State University, Bozeman, Montana, USA
[2]Space Science Applications Laboratory, The Aerospace Corporation, Los Angeles, California, USA
[3]The Johns Hopkins University Applied Physics Laboratory LLC, Laurel, Maryland, USA
[4]Institute for the Study of Earth, Oceans, and Space, University of New Hampshire, Durham, New Hampshire, USA
[5]Space Sciences Laboratory, UC Berkeley, Berkeley, California, USA

Key Points:

- The lat/lon scale sizes at LEO were 28.8 ± 0.8 km and 50.8 ± 11.4 km, respectively.
- Magnetic equator scale sizes are similar to the whistler-mode chorus source scale.

Corresponding author: Mykhaylo Shumko, msshumko@gmail.com

Abstract

The FIREBIRD-II CubeSats simultaneously observed a large microburst with multiple bounces on February 2nd, 2015 during a small storm. This is the first such microburst observed by two spacecraft, and it sheds light on its spatial scale sizes and bounce periods. Its lower bound latitudinal scale size was 28.8 ± 0.8 km and the longitudinal scale size was 50.8 ± 11.4 km in low earth orbit. Using the Tsyganenko 1989 magnetic field model, these scale sizes were mapped to the magnetic equator to get the radial and azimuthal scale sizes of at least 504 ± 14 km and 530 ± 119 km, respectively. These equatorial scale sizes are similar to the whistler-mode chorus wave source scale sizes, which further support the hypothesis that microbursts are a product of whistler-mode chorus waves scattering radiation belt electrons. Lastly, the electron bounce period from the subsequent bounces was calculated and compared to analytical and numerical bounce times to validate numerous magnetic field models.

1 Introduction

The dynamics of radiation belt electrons are complex, and are driven by competition between source and loss processes. A few possible loss processes are radial diffusion [*Shprits and Thorne*, 2004], magnetopause shadowing [*Ukhorskiy et al.*, 2006], and pitch angle diffusion [*Selesnick et al.*, 2003; *Abel and Thorne*, 1998] due to plasma wave and Coulomb scattering. As described in [*Millan and Thorne*, 2007; *Thorne*, 2010] and references contained within, there are a variety of waves that cause pitch angle scattering, including electromagnetic ion cyclotron waves, plasmaspheric hiss, and whistler-mode chorus. Whistler-mode chorus predominantly occurs in the dawn sector [*Li et al.*, 2009] where it accelerates electrons with large equatorial pitch angles and scatters electrons with small equatorial pitch angles [*Horne and Thorne*, 2003]. It is currently believed that chorus waves are responsible for microbursts, an intense increases in electron precipitation flux lasting $\sim 100\ ms$.

Microbursts were first termed by *Anderson and Milton* [1964] who used high altitude balloon observations of bremsstrahlung X-rays emitted from scattered microburst electrons in the atmosphere. Since then, microbursts have routinely been observed with other balloon missions [*Parks*, 1967; *Woodger et al.*, 2015; *Anderson et al.*, 2017] and in Low Earth Orbit (LEO) with, e.g. SAMPEX > 1 MeV energy channel [*Nakamura et al.*, 1995, 2000; *Blake et al.*, 1996; *Lorentzen et al.*, 2001a,b; *O'Brien et al.*, 2003, 2004; *Blum et al.*, 2015] and FIREBIRD-II with its > 200 keV energy channels [*Crew et al.*, 2016]. Similar to chorus waves, microbursts predominantly occur in the dawn sector [*Lorentzen et al.*, 2001b]. Un-

derstanding microburst precipitation is important to radiation belt dynamics since they have been modeled and empirically estimated to deplete the relativistic electron population of the outer radiation belt on time scales of hours to a few days [*O'Brien et al.*, 2004; *Thorne et al.*, 2005; *Shprits et al.*, 2007].

An important parameter in the estimation of instantaneous radiation belt electron losses due to microbursts is their scale size. *Parks* [1967] used balloon measurements of bremsstrahlung X-rays to estimate the scale size of predominantly low energy microbursts as 40 ± 14 km. In *Blake et al.* [1996], a microburst with multiple bounces was observed with SAMPEX was estimated to have a latitudinal scale size of "at least a few tens of kilometers", and concluded that typically they are less than a few tens of electron gyroradii in size. *Dietrich et al.* [2010] used SAMPEX along with ground-based very low frequency stations to conclude that microbursts have scale sizes less than 4 km.

Since February 1st, 2015, microbursts have been observed by FIREBIRD-II, a pair of CubeSats in LEO. On February 2nd, 2015, *Crew et al.* [2016] reported a microburst with a scale size greater than 11 km. On the same day, a microburst with multiple bounces was simultaneously observed on both spacecraft. The microburst decay was observed over the period of a few seconds, while the spacecraft were traveling predominantly in latitude. This analysis uses FIREBIRD-II to resolve the spatial and temporal properties of the first microburst with multiple bounces observed with two spacecraft. The rest of this paper is organized as follows: in section 2, the spacecraft and the microburst observation will be introduced. In section 3, the methodology of the spacecraft time and position correction, the microburst latitudinal and longitudinal scale sizes in LEO and the magnetic equator, and electron bounce period will be explained. Lastly, in section 4, these results will be tied to the current empirical and theoretical understanding of microbursts and their connection to whistler-mode chorus scales.

2 Spacecraft and Observation

FIREBIRD-II is an identically-instrumented pair of 1.5U CubeSats (FU3 and FU4), launched on January 31st, 2015. Their orbit has an apogee of 632 km and perigee of 433 km, and 99° inclination [*Crew et al.*, 2016]. FU3 and FU4 are flying in a string of pearls configuration with FU4 ahead, to resolve the space-time ambiguity inherent to single spacecraft missions such as SAMPEX.

Each FIREBIRD-II unit has a collimated and a surface solid state detector with complementary fields of view of 54° and 90°. They are observing electron precipitation in six energy channels from ~ 230 keV to > 1 MeV. The adjustable sampling rate is 18.75 ms by default and can be at a fast as 12.5 ms.

On February 2nd, 2015 at 06:12:53 UT, a microburst and subsequent bounces were observed simultaneously on both spacecraft. Figure 1 shows the electron flux data (HiRes) of the microburst. Five peaks were observed on both spacecraft. On the collimted detector, the microburst was seen up to the fourth energy channel (555 - 771 keV), while on the surface detector it was observed up to the fifth energy channel (683 - 950 keV). Only FU3 has a functioning surface detector, thus only data from the lowest four energy channels of the collimated detectors was used for this analysis. In addition, since FU4's 5th peak in the fourth energy channel was buried in Poisson noise, only the first four peaks were used in the spatial scale analysis.

The earliest peak was not dispersed, and subsequent peaks showed dispersion, which implies that this was a single microburst with subsequent decaying bounces. At this time, the spacecraft was above Sweden, latitude = 63°, longitude = 15°, altitude = 650 km, at the eastern edge of the bounce loss cone. For this analysis, the bounce loss cone is defined as the region where locally mirroring electrons will mirror at an altitude less than 100 km in the opposite hemisphere, and could be lost due to collisions in the atmosphere [*Abel and Thorne*, 1998]. For locally mirroring electrons, the mirror point in the opposite hemisphere was calculated to be 95 km using the Tsyganenko 1989 (T89) magnetic field model [*Tsyganenko*, 1989] with the IRBEM library. Roughly 40 - 60 % of the microburst electrons were lost at each bounce.

The geomagnetic conditions at the time were Kp = 4, and DST = -44 nT, during the transition between the main and recovery phases. Using the spacecraft location and geomagnetic conditions, the geomagnetic location at this time was McIlwain L = 4.7, MLT = 8.3, calculated using T89.

3 Analysis

3.1 Time and position correction

At the beginning of the FIREBIRD-II mission, their clocks were not synchronized and there was uncertainty in their separation. The approach to calculate their relative clock differ-

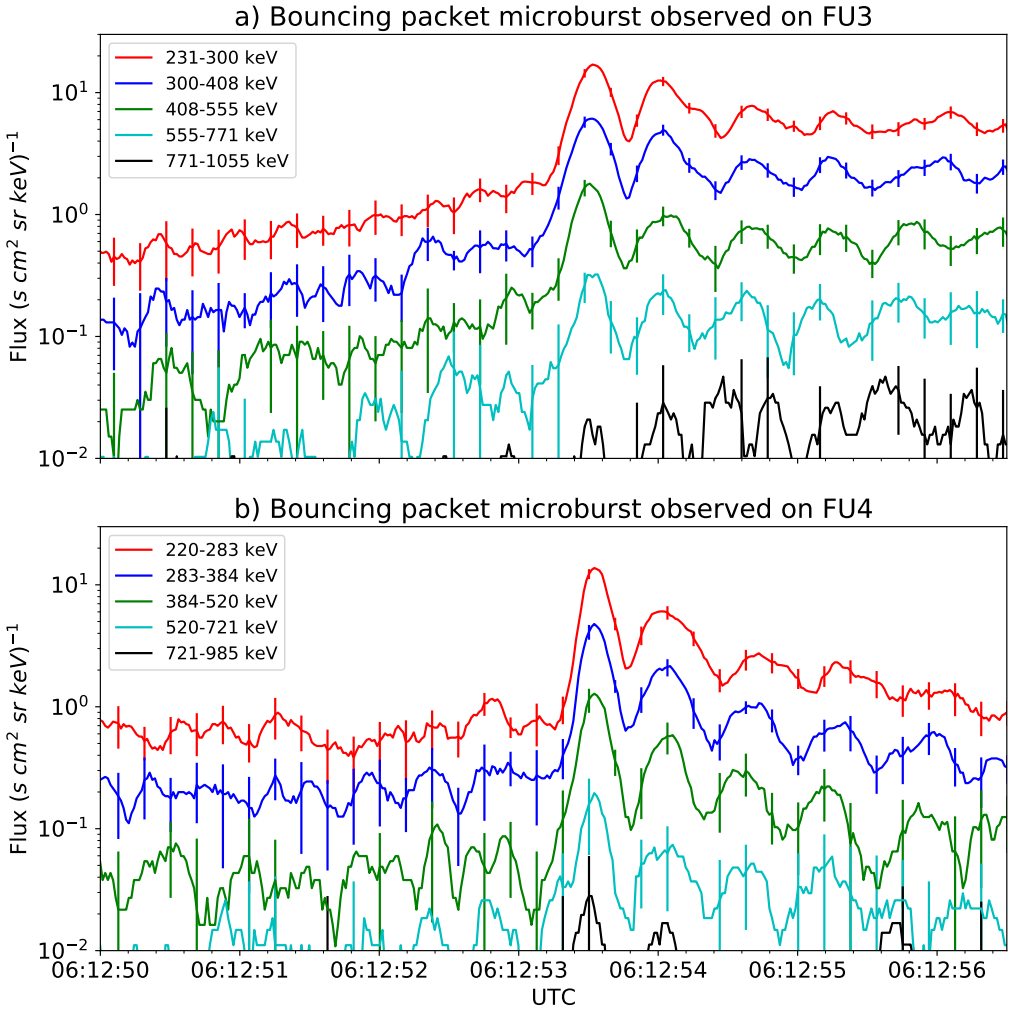

Figure 1. HiRes data of the microburst observed at February 2nd, 2015 at 06:12:53 UT, smoothed with a 150 ms window. The subsequent bounces showed little energy dispersion. As discussed in section 3 a time correction of -2.28 s was applied to FU3. While the flux from five energy channels is shown, only channels with reasonable counting statistics were used for the spatial scale analysis.

ence δt_c, is a cross-correlation time lag analysis on temporal events that are observed simultaneously, e.g. a train of identical microbursts seen on both spacecraft on the same day as the microburst in this case study.

Six time periods with coincident microbursts were hand-picked on February 2nd, 2015 for this analysis. The clock difference from the simultaneous microbursts was linearly fit to account for the clock drift ($\approx$ 20 ms/hour at this time) and it was $\delta t_c = 2.28 \pm 0.12\ s$ at the time of the microburst. This time shift was applied to the HiRes data in Fig. 1. To independently confirm the clock difference, it was also calculated using the time stamps of the FIREBIRD-II telemetry beacons during operational passes. Since they had a common time reference, the ground station computer, a time difference $\delta t_c = 2.45^{+0.51}_{-0.98}$ s was derived.

To calculate their separation, the data was first corrected for the clock difference, and the same cross-correlation time lag analysis was applied to spatial events that are assumed to be stationary. This time lag, δt_d for spatial events is the time it takes the trailing satellite to move to the leading satellite's position. This analysis yielded a time lag of $\delta t_d = 2.64 \pm 0.12$ s. With the Two Line Elements (TLE) derived spacecraft velocity, $v = 7.57\ km/s$, the calculated spacecraft separation was, $d = 19.9 \pm 0.9\ km$.

An independent method to confirm the spacecraft separation was developed. The separation was calculated using TLEs. The TLE released for February 2nd, was anomalous and was not used. Instead, seven TLEs released up to five days after the microburst event were backpropagated, using the SGP-4 algorithm [*Hoots and Roehrich*, 1980]. Then the predicted spacecraft separations at the time of the microburst event were averaged to derive a separation of $d = 18.4 \pm 1.5$ km. These two methods give similar results, which imply that the stationary event assumption used in the cross-correlation time lag analysis is a reasonable assumption.

3.2 Microburst Scale Sizes

Using the event and orbit topology shown in Fig. 2 and error propagated from the cross-correlation derived spacecraft separation, the latitudinal scale size is greater than 28.8$\pm$ 0.8 km. This scale size is represented by the latitudinal extent of the rectangles in Fig. 2.

Since magnetospheric electrons drift eastward and were seen for multiple bounces, it is possible to calculate the longitudinal scale size of the microburst. The distance that the electrons drift azimuthally in a single bounce is given by,

$$d_{az} = 2\pi(R_E + A)\cos(\lambda)\frac{t_b}{< T_d >} \tag{1}$$

where R_E is the Earth's radius, A is the spacecraft altitude, λ is the magnetic latitude, t_b is the electron bounce period, and $< T_d >$ is the electron drift period. *Parks* [2003] derived $< T_d >$ to be,

$$< T_d > \approx \begin{cases} 43.8/(L \cdot E) & \text{if } \alpha_0 = 90° \\ 62.7/(L \cdot E) & \text{if } \alpha_0 = 0° \end{cases} \tag{2}$$

where E is the electron energy in MeV, L is the L shell, and α_0 is the equatorial pitch angle. The valid limit for this analysis is $\alpha_0 = 0°$ since electrons mirroring at FIREBIRD-II have $\alpha_0 \approx 3.7°$.

The microburst's longitudinal scale size was the furthest distance that its electrons drifted east and were last seen. This was calculated with $D_{az} = n\, d_{az}$ where n is the number of bounces observed. Using this methodology, the longitudinal scale size was greater than 38.5 ± 8.8 km for the 555 keV electrons and greater than 50.8 ± 11.4 km for the 771 keV electrons shown with the red dashed box in Fig. 2. The stars with energy labels in Fig. 2 represent the locations of electrons with that energy when the microburst was seen at the first peak (P1), and drifted eastward to be last seen at P5 for FU3 and P4 for FU4.

The longitudinal and latitudinal scale sizes at LEO were mapped to the magnetic equator using the T89 magnetic field model. The radial scale size (latitudinal scale mapped from LEO) is greater than 504 ± 14 km and azimuthal scale size (longitudinal scale mapped from LEO) of 555 keV electrons is greater than 451 ± 103 km and of 771 keV electrons is greater than 530 ± 119 km.

3.3 Electron Bounce Period

Lastly, the observed bounce period, t_b as a function of energy was calculated. To calculate the observed t_b and uncertainties, the raw HiRes flux was baseline-subtracted and fitted. The baseline flux is defined in *O'Brien et al.* [2004] as the flux at the 10th percentile over a specified time interval, half second for this analysis. The flux was fitted with multiple superposed Gaussians. The flux uncertainty is from the Poisson errors of microburst and

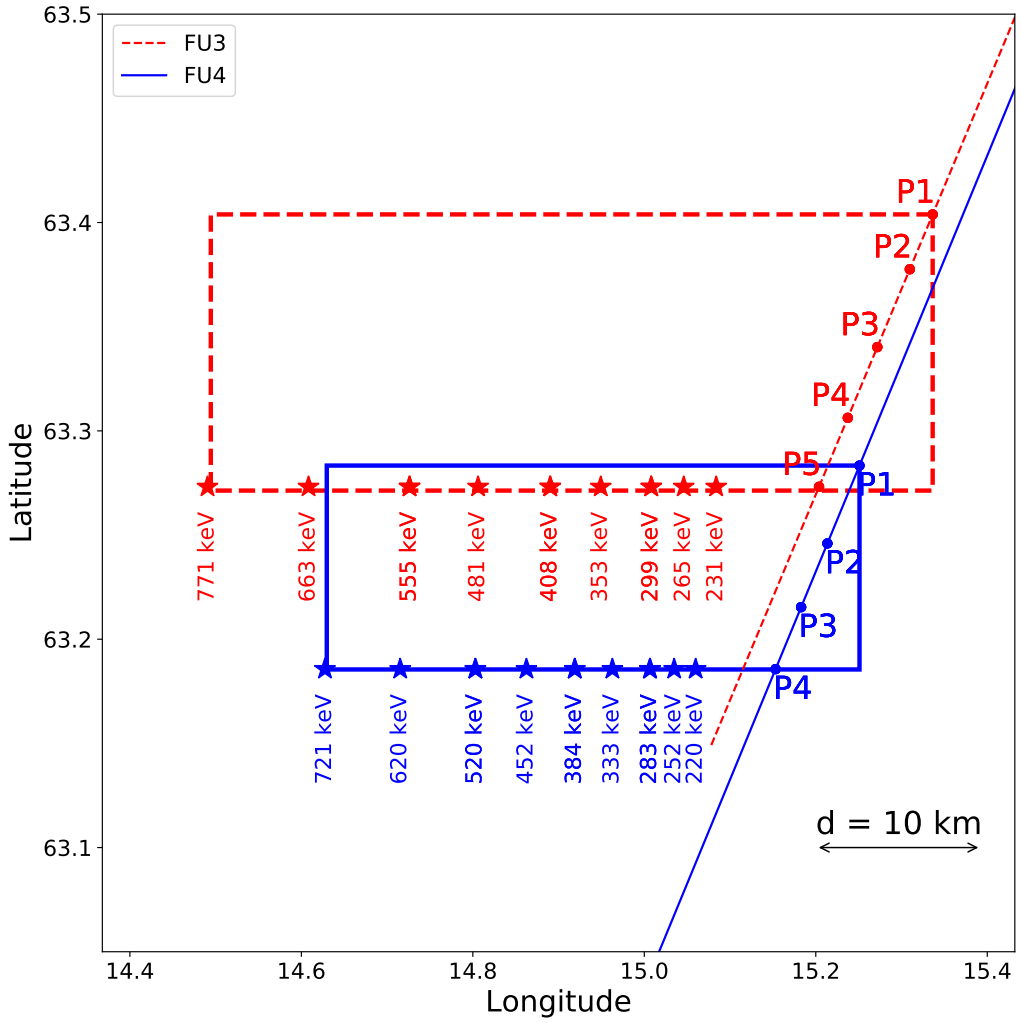

Figure 2. The topology of the FIREBIRD-II orbit and the multiple bounces of the microburst projected onto latitude and longitude with axis scaled to equal distance. Attributes relating to FU3 shown in red dashed lines, and FU4 with blue solid lines. The spacecraft path is shown with the diagonal lines, starting at the upper right corner. The labels P(N) indicate where the spacecraft were when the N^{th} peak was seen in the lowest energy channel in the HiRes data. The stars with the accompanying energy labels represent the locations of the electrons with that energy that started at time of P1, and were seen at the last peak on each spacecraft. The rectangles represent the lower bound of the microburst scale size, assuming that the majority of the electrons were in the upper boundary of energy channel 4.

baseline fluxes summed in quadrature. Using the fit parameters, the mean t_b for the lowest four energy channels was calculated and shown in Fig. 3 with green and purple rectangles.

The bounces observed with FU3 were biased to earlier times in the lowest two energy channels. This hints at the underlying distribution of electron flux within the energy channel, and suggests that there were more electrons at the higher energy end. A Gaussian fit cannot account for this bias, and as a first order correction, minima between peaks was used to calculate t_b, and is shown in Fig. 3 with blue rectangles.

Superposed on Fig. 3, are t_b curves for various models including an analytical solution from *Schulz and Lanzerotti* [1974], and numerical models: T89, Tsyganenko 2004 (T04) [*Tsyganenko and Sitnov*, 2005], and Olson & Pfitzer Quiet [*Olson and Pfitzer*, 1982]. The numerical t_b curves were calculated using a Python wrapper for IRBEM. It traces the magnetic field line between mirror points, to calculate t_b assuming conservation of energy and the first adiabatic invariant for electrons mirroring at FIREBIRD-II.

4 Discussion

The scale sizes reported in section 3.2 were a lower bound. They were larger than the latitudinal scale size reported in *Blake et al.* [1996], and similar to the scale size reported in *Parks* [1967]. Furthermore, the latitudinal scale size in this study was roughly $\sim$ 2.6 times larger than other simultaneous microbursts reported in *Crew et al.* [2016] and $\sim$ 10 times larger than than reported in *Dietrich et al.* [2010]. No energy dependence on the scale size was observed.

From section 3.2, the microburst scale size at the magnetic equator was similar to the whistler-mode chorus source scale sizes reported in *Agapitov et al.* [2011, 2017]. In *Agapitov et al.* [2011], chorus source scale scales of $\sim$ 600 km were observed by CLUSTER at $L \sim$ 4.5. In *Agapitov et al.* [2017], The Van Allen Probes were used to measure source scale sizes of $\sim$ 500 and $\sim$ 800 km for upper and lower band chorus, respectively. Using the evidence from this analysis, this microburst was most likely scattered by a whistler-mode chorus.

Using the fit parameters from section 3.3, the exponential E-folding energy, E_0 was calculated to be $E_0 \sim 100\ keV$. This is similar to the results in *Lee et al.* [2005] who used STSAT-1 and *Datta et al.* [1997] who used a sounding rocket. It is soft for a typical microburst observed with FIREBIRD-II. Since the microburst was seen up to the 683-950 keV energy channel on the surface detector, a more realistic longitudinal scale size may be that

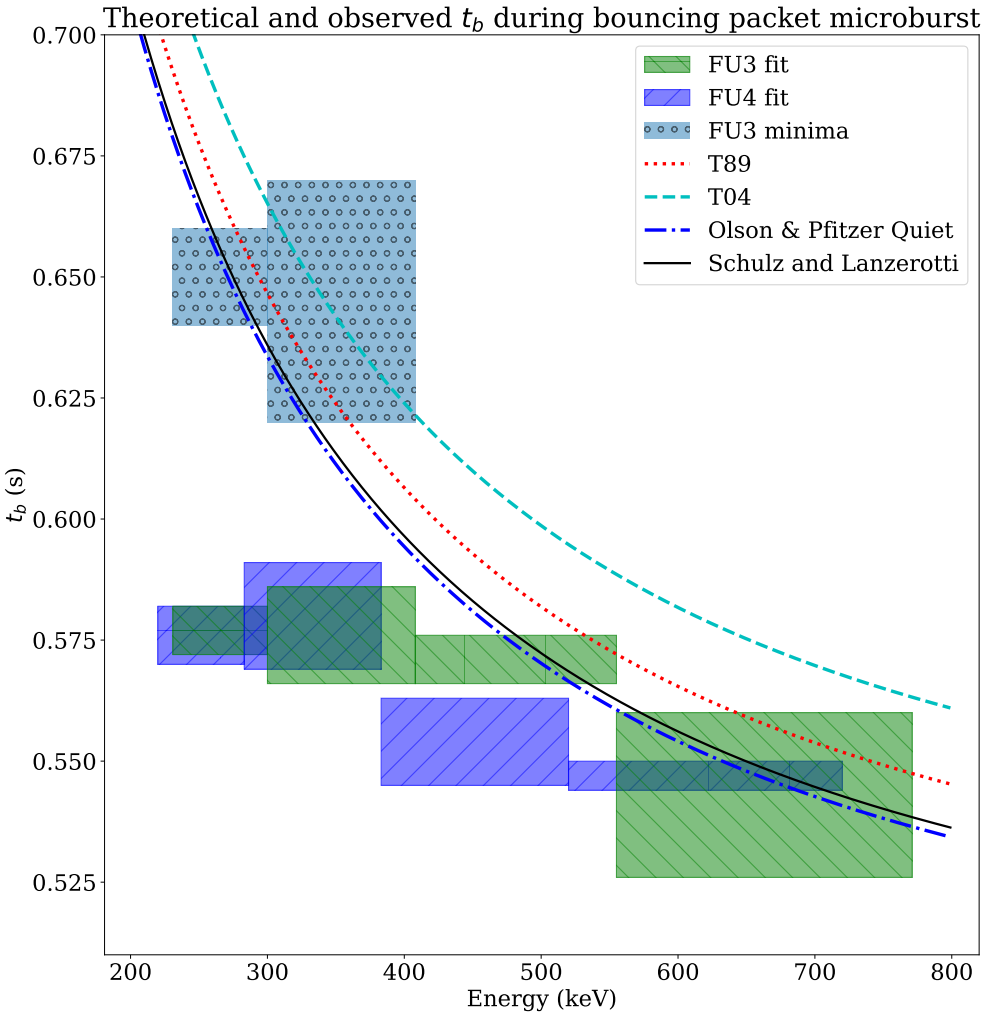

Figure 3. Observed and theoretical t_b for electrons of energies from 200 to 770 keV. The solid black line is t_b in a dipole magnetic field, derived in *Schulz and Lanzerotti* [1974]. The red and cyan dashed lines are the t_b derived using the T89, and T04 magnetic field models with IRBEM. Lastly, the blue dashed curve is the t_b derived using the Olson & Pfitzer Quiet model. The green and purple rectangles represent the observed t_b for FU3 and FU4 using a Gaussian fit, respectively. The blue rectangles represent the observed t_b calculated with the minima between the bounces. The width of the boxes represent the width of those energy channels, and the height represents the uncertainty from the fit.

of the 771 keV electrons. There was no statistically significant change in E_0 for subsequent bounces.

Lastly, the fitted, high energy t_b shown in Fig. 3 agrees to most models but has the largest discrepancy at lower energies. This discrepancy is removed by using the minima to calculate t_b for the < 555 keV peaks.

5 Conclusions

This was a first observation of a large microburst with multiple bounces by two spacecraft. Its lower bound LEO latitudinal and longitudinal scale sizes of 28.8 ± 0.8 km and 50.8 ± 11.4 km make it one of the largest observed. No energy dependence on the scale size was observed. Furthermore, its LEO scale sizes mapped to the magnetic equator were 504 ± 14 km radially and 530 ± 119 km azimuthally, similar to the whistler-mode chorus source region scale size reported in previous literature. The similarity of the microburst and chorus source region scale sizes, as well as magnetospheric location and condition, support the idea that microbursts are scattered by whistler-mode chorus.

Lastly, the Gaussian fitted and theoretical bounce periods agree at high energies, but disagree by as much as ∼ 20% at the lowest energies that FIREBIRD-II observes. This is partially due to the bias to earlier times in the peaks for the two lowest energy channels, and it hints at the underlying energy-dependent electron flux spectra. By using the minima method to calculate t_b, there is better agreement for those energy channels.

Acknowledgments

This work was made possible with help from the FIREBIRD team, and the members of the Space Sciences and Engineering Laboratory at Montana State University for their hard work to make this mission a success. In addition, I acknowledge Drew Turner for his suggestions regarding the bounce period calculations. The FIREBIRD-II data are available at http://solar.physics.montana.edu/FIREBIRD_II/. This material is based upon work at Montana State University supported by the National Science Foundation under Grant Numbers 0838034 and 1339414.

References

Abel, B., and R. M. Thorne (1998), Electron scattering loss in earth's inner magnetosphere: 1. dominant physical processes, *Journal of Geophysical Research: Space Physics*, *103*(A2), 2385–2396.

Agapitov, O., V. Krasnoselskikh, T. Dudok de Wit, Y. Khotyaintsev, J. S. Pickett, O. Santolik, and G. Rolland (2011), Multispacecraft observations of chorus emissions as a tool for the plasma density fluctuations' remote sensing, *Journal of Geophysical Research: Space Physics*, *116*(A9), n/a–n/a, doi:10.1029/2011JA016540, a09222.

Agapitov, O., L. W. Blum, F. S. Mozer, J. W. Bonnell, and J. Wygant (2017), Chorus whistler wave source scales as determined from multipoint van allen probe measurements, *Geophysical Research Letters*, pp. n/a–n/a, doi:10.1002/2017GL072701, 2017GL072701.

Anderson, B., S. Shekhar, R. Millan, A. Crew, H. Spence, D. Klumpar, J. Blake, T. O'Brien, and D. Turner (2017), Spatial scale and duration of one microburst region on 13 august 2015, *Journal of Geophysical Research: Space Physics*.

Anderson, K. A., and D. W. Milton (1964), Balloon observations of x rays in the auroral zone: 3. high time resolution studies, *Journal of Geophysical Research*, *69*(21), 4457–4479, doi:10.1029/JZ069i021p04457.

Blake, J., M. Looper, D. Baker, R. Nakamura, B. Klecker, and D. Hovestadt (1996), New high temporal and spatial resolution measurements by sampex of the precipitation of relativistic electrons, *Advances in Space Research*, *18*(8), 171 – 186, doi:http://dx.doi.org/10.1016/0273-1177(95)00969-8.

Blum, L., X. Li, and M. Denton (2015), Rapid mev electron precipitation as observed by sampex/hilt during high-speed stream-driven storms, *Journal of Geophysical Research: Space Physics*, *120*(5), 3783–3794, doi:10.1002/2014JA020633, 2014JA020633.

Crew, A. B., H. E. Spence, J. B. Blake, D. M. Klumpar, B. A. Larsen, T. P. O'Brien, S. Driscoll, M. Handley, J. Legere, S. Longworth, K. Mashburn, E. Mosleh, N. Ryhajlo, S. Smith, L. Springer, and M. Widholm (2016), First multipoint in situ observations of electron microbursts: Initial results from the nsf firebird ii mission, *Journal of Geophysical Research: Space Physics*, *121*(6), 5272–5283, doi:10.1002/2016JA022485, 2016JA022485.

Datta, S., R. Skoug, M. McCarthy, and G. Parks (1997), Modeling of microburst electron precipitation using pitch angle diffusion theory, *Journal of Geophysical Research: Space Physics*, *102*(A8), 17,325–17,333.

Dietrich, S., C. J. Rodger, M. A. Clilverd, J. Bortnik, and T. Raita (2010), Relativistic microburst storm characteristics: Combined satellite and ground-based observations, *Journal of Geophysical Research: Space Physics*, *115*(A12).

Hoots, F. R., and R. L. Roehrich (1980), Models for propagation of norad element sets, *Tech. Rep. 3*, Spacetrack.

Horne, R. B., and R. M. Thorne (2003), Relativistic electron acceleration and precipitation during resonant interactions with whistler-mode chorus, *Geophysical Research Letters*, *30*(10), n/a–n/a, doi:10.1029/2003GL016973, 1527.

Lee, J.-J., G. K. Parks, K. W. Min, H. J. Kim, J. Park, J. Hwang, M. P. McCarthy, E. Lee, K. S. Ryu, J. T. Lim, E. S. Sim, H. W. Lee, K. I. Kang, and H. Y. Park (2005), Energy spectra of 170-360 kev electron microbursts measured by the korean stsat-1, *Geophysical Research Letters*, *32*(13), doi:10.1029/2005GL022996, l13106.

Li, W., R. M. Thorne, V. Angelopoulos, J. Bortnik, C. M. Cully, B. Ni, O. LeContel, A. Roux, U. Auster, and W. Magnes (2009), Global distribution of whistler-mode chorus waves observed on the themis spacecraft, *Geophysical Research Letters*, *36*(9), n/a–n/a, doi:10.1029/2009GL037595, l09104.

Lorentzen, K. R., J. B. Blake, U. S. Inan, and J. Bortnik (2001a), Observations of relativistic electron microbursts in association with vlf chorus, *Journal of Geophysical Research: Space Physics*, *106*(A4), 6017–6027, doi:10.1029/2000JA003018.

Lorentzen, K. R., M. D. Looper, and J. B. Blake (2001b), Relativistic electron microbursts during the gem storms, *Geophysical Research Letters*, *28*(13), 2573–2576, doi:10.1029/2001GL012926.

Millan, R., and R. Thorne (2007), Review of radiation belt relativistic electron losses, *Journal of Atmospheric and Solar-Terrestrial Physics*, *69*(3), 362 – 377, doi:http://dx.doi.org/10.1016/j.jastp.2006.06.019, global Aspects of Magnetosphere-Ionosphere CouplingGlobal Aspects of Magnetosphere-Ionosphere Coupling.

Nakamura, R., D. N. Baker, J. B. Blake, S. Kanekal, B. Klecker, and D. Hovestadt (1995), Relativistic electron precipitation enhancements near the outer edge of the radiation belt, *Geophysical Research Letters*, *22*(9), 1129–1132, doi:10.1029/95GL00378.

Nakamura, R., M. Isowa, Y. Kamide, D. Baker, J. Blake, and M. Looper (2000), Observations of relativistic electron microbursts in association with vlf chorus, *J. Geophys. Res*, *105*, 15,875–15,885.

O'Brien, T. P., K. R. Lorentzen, I. R. Mann, N. P. Meredith, J. B. Blake, J. F. Fennell, M. D. Looper, D. K. Milling, and R. R. Anderson (2003), Energization of relativistic electrons in the presence of ulf power and mev microbursts: Evidence for dual ulf and vlf acceleration, *Journal of Geophysical Research: Space Physics*, *108*(A8), n/a–n/a, doi: 10.1029/2002JA009784, 1329.

O'Brien, T. P., M. D. Looper, and J. B. Blake (2004), Quantification of relativistic electron microburst losses during the gem storms, *Geophysical Research Letters*, *31*(4), n/a–n/a, doi:10.1029/2003GL018621, l04802.

Oliven, M. N., and D. A. Gurnett (1968), Microburst phenomena: 3. an association between microbursts and vlf chorus, *Journal of Geophysical Research*, *73*(7), 2355–2362, doi: 10.1029/JA073i007p02355.

Olson, W. P., and K. A. Pfitzer (1982), A dynamic model of the magnetospheric magnetic and electric fields for july 29, 1977, *Journal of Geophysical Research: Space Physics*, *87*(A8), 5943–5948, doi:10.1029/JA087iA08p05943.

Parks, G. (2003), *Physics Of Space Plasmas: An Introduction, Second Edition*, Westview Press.

Parks, G. K. (1967), Spatial characteristics of auroral-zone x-ray microbursts, *Journal of Geophysical Research*, *72*(1), 215–226.

Schulz, M., and L. J. Lanzerotti (1974), *Particle Diffusion in the Radiation Belts*, Springer.

Selesnick, R. S., J. B. Blake, and R. A. Mewaldt (2003), Atmospheric losses of radiation belt electrons, *Journal of Geophysical Research: Space Physics*, *108*(A12), doi: 10.1029/2003JA010160, 1468.

Shprits, Y. Y., and R. M. Thorne (2004), Time dependent radial diffusion modeling of relativistic electrons with realistic loss rates, *Geophysical Research Letters*, *31*(8), n/a–n/a, doi:10.1029/2004GL019591, l08805.

Shprits, Y. Y., N. P. Meredith, and R. M. Thorne (2007), Parameterization of radiation belt electron loss timescales due to interactions with chorus waves, *Geophysical Research Letters*, *34*(11), n/a–n/a, doi:10.1029/2006GL029050, l11110.

Thorne, R. M. (2010), Radiation belt dynamics: The importance of wave-particle interactions, *Geophysical Research Letters*, *37*(22), doi:10.1029/2010GL044990, l22107.

Thorne, R. M., T. P. O'Brien, Y. Y. Shprits, D. Summers, and R. B. Horne (2005), Timescale for mev electron microburst loss during geomagnetic storms, *Journal of Geophysical Research: Space Physics*, *110*(A9), n/a–n/a, doi:10.1029/2004JA010882, a09202.

Tsyganenko, N. (1989), A solution of the chapman-ferraro problem for an ellipsoidal magnetopause, *Planetary and Space Science*, *37*(9), 1037 – 1046, doi: http://dx.doi.org/10.1016/0032-0633(89)90076-7.

Tsyganenko, N. A., and M. I. Sitnov (2005), Modeling the dynamics of the inner magnetosphere during strong geomagnetic storms, *Journal of Geophysical Research: Space Physics*, *110*(A3), n/a–n/a, doi:10.1029/2004JA010798, a03208.

Ukhorskiy, A. Y., B. J. Anderson, P. C. Brandt, and N. A. Tsyganenko (2006), Storm time evolution of the outer radiation belt: Transport and losses, *Journal of Geophysical Research: Space Physics*, *111*(A11), n/a–n/a, doi:10.1029/2006JA011690, a11S03.

Woodger, L., A. Halford, R. Millan, M. McCarthy, D. Smith, G. Bowers, J. Sample, B. Anderson, and X. Liang (2015), A summary of the barrel campaigns: Technique for studying electron precipitation, *Journal of Geophysical Research: Space Physics*, *120*(6), 4922–4935.